Spiral Waveguides on Germanium-on-Silicon Nitride Platform for Mid-IR Sensing Applications
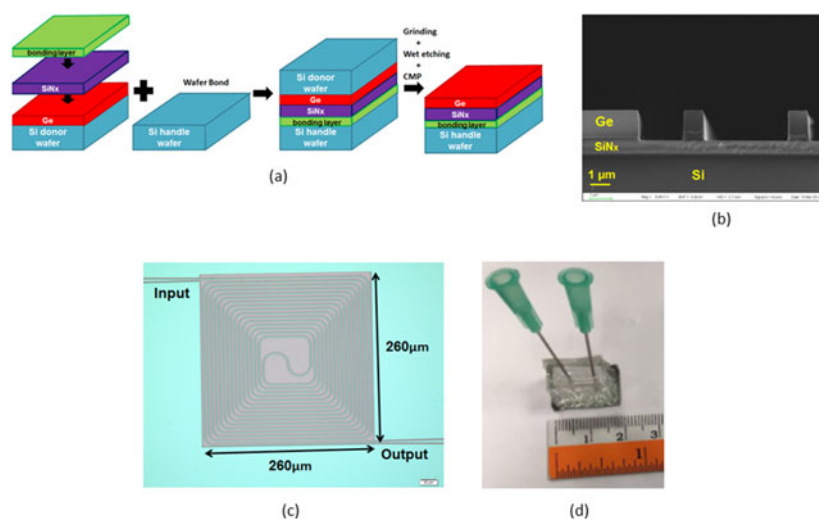
Wei Li
P. Anantha
Kwang Hong Lee
Hao Dong Qiu
Xin Guo
Simon Chun Kiat Goh
Lin Zhang
Hong Wang
Richard A. Soref
Chuan Seng Tan

Spiral Waveguides on Germanium-on-Silicon Nitride Platform for Mid-IR Sensing Applications

Wei Li [ID],[1] **P. Anantha,**[1] **Kwang Hong Lee** [ID],[2] **Hao Dong Qiu,**[1]
Xin Guo,[1] **Simon Chun Kiat Goh,**[1] **Lin Zhang,**[1] **Hong Wang** [ID],[1]
Richard A. Soref [ID],[3] **and Chuan Seng Tan** [ID] [1,2]

[1]School of Electrical and Electronic Engineering, Nanyang Technological University,
Singapore 639798, Singapore
[2]Low Energy Electronic System, Singapore-MIT Alliance for Research and Technology,
Singapore 138602, Singapore
[3]Department of Engineering, University of Massachusetts at Boston, Boston,
MA 02125, USA

Abstract: Spiral waveguides on a new germanium-on-silicon nitride (GON) platform with a wide transparency and a large core-clad index contrast for mid-infrared (mid-IR) sensing applications are demonstrated. Spiral waveguide sensors with a low bending loss on this platform enable compact sensors for mid-IR absorption spectroscopy. A minimum volumetric concentration of 5% isopropanol (IPA) in an IPA–acetone mixture is measured. This detection limit is three times lower than the counterpart waveguide, fabricated on the regular germanium-on-silicon platform with similar propagation loss at 3.73 μm wavelength. This silicon-compatible GON sensor is promising for applications such as environmental studies, industrial leak detection, process control, medical breath analysis, and many more.

Index Terms: Integrated optics devices, integrated optics materials, sensor, waveguides, absorption.

1. Introduction

Group-IV photonics is intensively studied in the recent years due to its compatibility with silicon processes, small footprint, low fabrication cost, immunity to electromagnetic interference, as well as its sensing applications in the mid-infrared (mid-IR) [1]. In particular, the mid-IR spectrum represents a primary spectral range for photonic sensing applications, as characteristic absorption fingerprints of most molecules reside here. Waveguide sensors are especially useful in the mid-IR because of their relative simplicity and accuracy. It is based on the interaction of the evanescent field of a waveguide mode with the surrounding media and the resulting perturbation of the intensity of the mode at the output end of the waveguide. Besides waveguide sensors, the recently reported mid-infrared spectroscopy using frequency comb has also explored a novel way to mid-IR sensing [2], [3]. These devices provide a promising method for the label-free detection of target molecules as well as for the real-time monitoring of solutions, gases, or reactions that occur near the device

surface. Unlike the conventional Fourier Transform Infrared Spectroscopy (FTIR) that is limited for use in laboratories due to its large size, these devices are small in size and require a minimal sample test volume. The reported mid-IR strip waveguides for laser spectroscopy has a 1,000 times higher sensitivity than FTIR in the liquid environment [4]. Thus these devices will have major impact on environment studies (e.g., detection of hazardous and greenhouse gases), industrial leak detection, process control, food processing, medical breath analysis, etc. [5].

The most commonly used platform— silicon-on-insulator (SOI) is not suitable for mid-IR sensing application since the material loss of the buried oxide layer becomes significant at 3.7 μm and beyond [6]. There are two commonly explored methods: bottom clad replacement or a new stack of mid-IR transparent material. To replace SiO_2 many candidates such as suspended silicon [7]–[9], silicon-on-sapphire [10]–[12], silicon-on-porous silicon [13] have been studied. The examples of new material stack include germanium-on-silicon (GOS) [14], [15], germanium-on-SOI [16], III-V semiconductors [17], [18], and newly reported germanium-on-glass [19]. Substantial efforts have been made to extend the operating wavelength to the mid-IR and impressive results have been obtained using GOS platform [20]–[22]. However, limited experimental demonstrations of mid-IR sensing applications have been reported. Besides, the replacement of bottom clad usually requires additional steps to remove the bottom clad layer like wet etching to remove SiO_2 to form suspended silicon, and new material stack like germanium-on-silicon does not provide a high core-clad index contrast ($\Delta n = 0.6$ for Ge/Si at 3.73 μm) thus making it challenging to realize compact waveguide sensors. In order to take the advantage of the wide transparency of germanium, and also to provide a large core-clad index contrast, we fabricate a new germanium based platform—germanium-on-silicon nitride (GON) for mid-IR sensing applications with a refractive index contrast ($\Delta n = 2.1$) close to that of SOI. This enables bent waveguides to achieve low bending loss even at small radius. Using silicon nitride as the under cladding layer has been reported before like silicon-on-silicon nitride (SON) but GON can further extend the operation wavelength and provide a larger index contrast than SON [23], [24].

According to equation (1) described below [25], the number density of molecules per unit volume is inversely proportional to the effective length of the waveguide and the absorption cross section of the evanescent field.

$$N_{min} = (dI/dI_0)\,/S(u)L \tag{1}$$

where dI/dI_0 is the fractional change in light intensity that can be detected, L is the effective absorption path length, and $S(\upsilon)$ is the absorption cross section of evanescent field. As can be seen from equation (1), the longer the effective absorption path length, the lower the number density that can be detected, thus the higher the sensitivity. For effective analysis, the length of the waveguide should normally be several millimeters or even longer. In both reports [10] and [12], straight strip waveguides were used as the sensor part to demonstrate the feasibility of using waveguides for absorption based sensing applications. However, the straight waveguides would consume a large dimension on chip in order to have a relatively higher sensitivity. If one introduces bends to the waveguide, the size of the sensor can be further reduced making it more compact and compatible with lab-on-chip applications. The refractive index contrast of GOS and SOS is smaller than that of SOI resulting in a higher bending loss which makes these two platforms not suitable for designing compact spiral waveguides for sensing applications. High evanescent field fraction will also contribute to the improvement of the sensitivity but may cause high propagation loss.

In this paper, we first present the fabrication of GON engineered wafer followed by utilizing this structure to design and demonstrate compact spiral waveguides for sensing applications. A fluidic chamber is integrated with the spiral waveguides to demonstrate the detection of isopropanol, a commonly used organic solvent in the semiconductor industry.

2. Wafer and Device Fabrication

GON wafer is realized by wafer bonding and layer transfer technique which provides a germanium layer free of misfit dislocations and is scalable to any wafer sizes. Two wafers are utilized in the
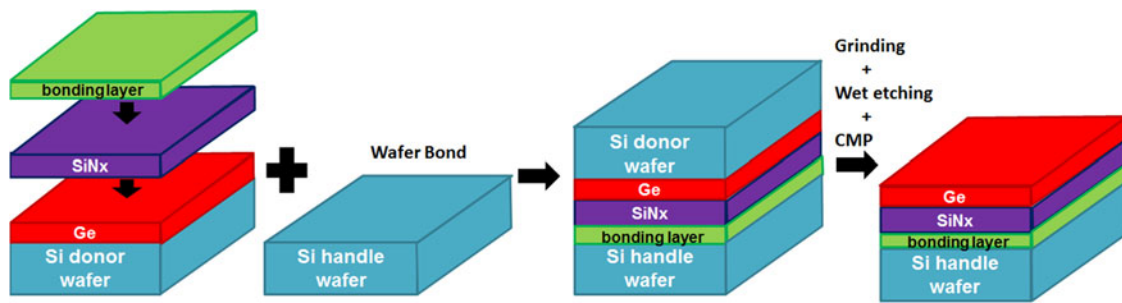
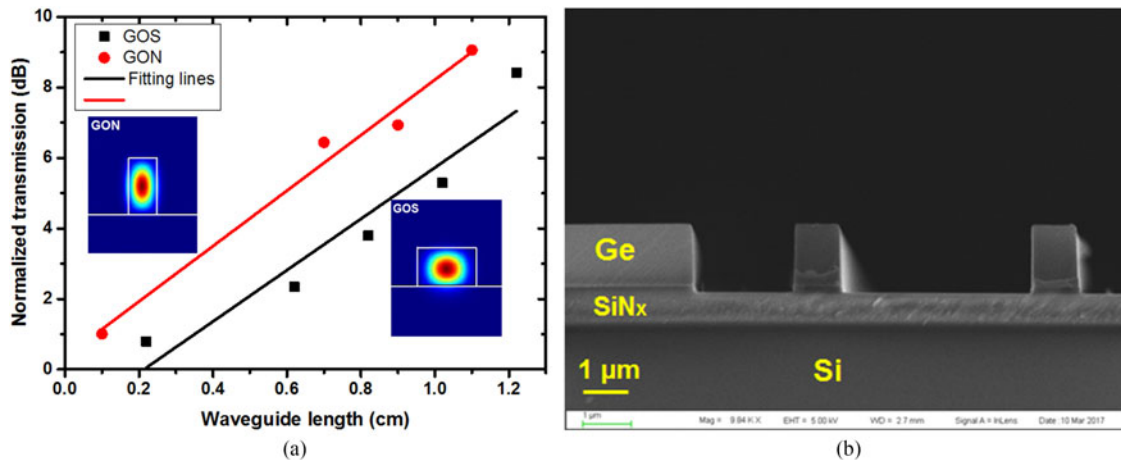Fig. 1. Schematic flow of the fabrication of GON wafer.

Fig. 2. (a) The cross sectional dimension of waveguides on GON is 1 μm width and 1.5 μm height; while the dimension of waveguides on GOS is 2 μm width and 1 μm height. The propagation losses of waveguides on GOS and GON are 7.28 $\pm$ 1.26 dB/cm and 7.86 $\pm$ 0.7 dB/cm respectively. The insets show the mode profiles of waveguides on the two platforms. (b) The cross-sectional SEM image of the waveguides fabricated on GON platform.

process: Si donor wafer and Si handle wafer. A high-quality crystalline Ge layer is grown on the Si donor wafer and followed by the deposition of SiN$_x$ on the Ge layer. Subsequently, a bonding layer is deposited on the SiN$_x$ layer to facilitate the wafer bonding process. The Si donor wafer is bonded onto the Si handle wafer followed by mechanical grinding and selective wet etching to remove the donor wafer completely. Chemical mechanical polishing (CMP) is used to remove the defects and Ge/Si intermixed layer on the exposed Ge epi-layer. All the materials used in this process are also commonly used in the semiconductor industry and thus the process is fully CMOS compatible. The fabrication process flow is summarised in Fig. 1. The details of GON fabrication process and the characterization of the final Ge layer can be found in ref [26].

The final GON structure used in this work comprises of a 1.5 μm thick Ge layer on 800 nm SiN$_x$. Lumerical MODE SOLUTION is used to determine the cross sectional dimension of the spiral waveguides on GON platform. In order to extend the evanescent field fraction to achieve a higher sensitivity, waveguides with a height of 1.5 μm and a width of 1 μm for single TE mode [19] are designed. In addition, waveguides on GOS platform with a height of 1 μm and a width of 2 μm for single TE mode are also designed for comparison to obtain a similar propagation loss as the waveguides on GON. According to the simulation results, the evanescent field fraction of waveguides on GON (12.8%) is about three times larger than that of GOS (4.4%) at the wavelength of 3.73 μm. The mode profiles of GON and GOS are shown in the inset of Fig. 2(a). The fabrication of these waveguides on GON and GOS, respectively, was carried out using electron-beam lithography and deep-reactive ion etching using sulfur hexaflouride (SF$_6$) as the etchant. The etching profile
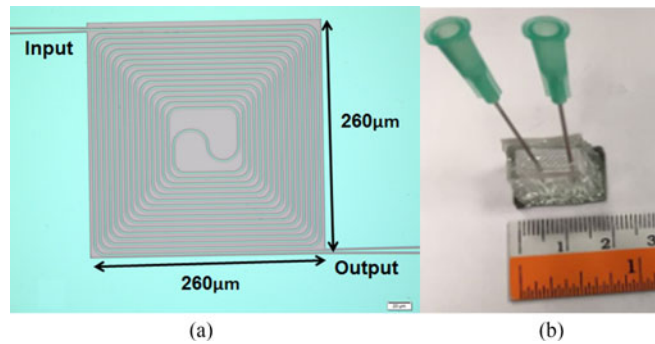
Fig. 3. (a) Top view of the spiral waveguide and (b) Ge spiral waveguide sensor chip bonded to the fluidic chamber (GON wafer).

of waveguides on GON is shown in Fig. 2(b). The propagation losses of waveguides on these two platforms are measured using the cut-back method and the results are shown in Fig. 2(a).

The propagation loss of waveguides on GON is 7.86 dB/cm which is almost the same as the loss of waveguides on GOS (7.28 dB/cm) despite its higher evanescent field fraction. This is mainly due to the higher core-clad index contrast of the GON platform resulting in a better mode confinement at the core/under-clad interface than that of the GOS wafer. Besides, the misfit dislocations have been removed through the layer transfer process resulting in a lower scattering loss. The similar propagation loss can rule out its influence on the sensitivity and only keep evanescent field fraction as the dominant variable.

The radii of the bent waveguides are determined by MODE SOLUTION simulation. The radii of 30 μm is chosen for bent waveguide on GON and 200 μm for GOS as the bending losses of the spiral waveguides on the two platforms are comparable and negligible at these two radii. This demonstrates one of the advantages of the GON platform that the large core-clad index contrast allows for a compact waveguide design suitable for lab-on-chip applications.

Spiral waveguides were designed on GON with an areal size of 260 μm by 260 μm and a total length of 4.02 mm so the total loss is 3.14 dB which is acceptable to our testing system. The gap between two adjacent waveguides is 5 μm, large enough to prevent the directional coupling. The top view of the spiral waveguide on GON is shown in Fig. 3(a) as seen from an optical microscope. Spiral waveguides with the same length were also fabricated on the GOS platform, where the radius of the bent waveguide is larger than that of waveguides on GON resulting in a much larger total area (600 μm $\times$ 600 μm). Fluidic chamber made of PDMS [27] was fabricated by 3D printing and integrated with the sensor chip. The PDMS chamber was first cured at 90 °C for 15 min and subsequently placed onto the sensor chip sealed with liquid PDMS and cured again. The PDMS has a strong absorption peak around the wavelength of 3.4 μm and its absorbance at 3.73 μm wavelength can be ignored [28]. A syringe pump system for liquid sample handling was also integrated with the chamber.

3. Experiment and Results

The liquid that is used to demonstrate the feasibility of the spiral waveguide sensor is isopropanol, also known as IPA. This organic liquid is commonly used in the semiconductor industry for cleaning wafers and has an absorption coefficient of about 144 cm^{-1} at 3.73 μm [29]. Acetone is used as the solvent and its absorption is negligible as the transmittance of acetone is about 100% at this wavelength. The absorption (in dB), A, induced by IPA in the fluidic chamber is calculated by considering the ratio of light intensity transmitted through the waveguide surrounded by pure acetone ($I_{solvent}$) and by a solution of IPA and acetone ($I_{analyte}$), defined as:

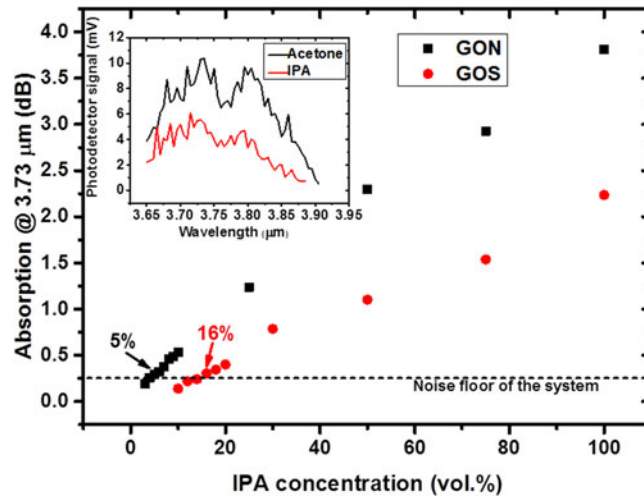$$A = 10\log_{10}\frac{I_{solvent}}{I_{analyte}} \qquad (2)$$

Fig. 4. Absorption of spiral waveguide sensor at different IPA-acetone mixtures. The lowest volumetric concentration of IPA that can be measured by the sensor on GON is 5% while for GOS platform it is 16%. Inset: Waveguide output for laser scan with acetone and IPA as the analytes.

The sensor chip was mounted on a *XYZ* translational stage with a vacuum chuck. Light source with a 3.73 μm wavelength from a rapid scan continuous wave (CW)-pulsed quantum cascade laser from DAYLIGHT SOLUTIONS, after going through a polarization controller, was then butt-coupled in and out of the spiral waveguide using a pair of single mode ZrF_4 fibers from Thorlabs. TE mode measurements were used similar to the simulations. The same waveguide was used throughout the experiment to eliminate any non-uniformity issue associated with waveguide intrinsic loss. For each measurement, a 0.4 mL solution was injected with different volumetric concentration of IPA into the chamber and removed with the syringe after a successful measurement. The chip was realigned for maximum output before the subsequent measurement. The output signals were measured with a high sensitivity InSb photodetector (-40 dB) from HORIBA. The same process has been repeated on the waveguide sensor on GOS platform as a benchmark.

In the current model adopted, the minimum detectable volumetric concentration of the analyte from the waveguide evanescent sensors can be derived by comparing the sensor signal to noise. Thus it is given as follows [30]:

$$C_{\min} = \frac{\sqrt{2}}{L\,\alpha\eta}\sqrt{\left(\frac{\Delta I_0}{I_0}\right)^2 + \left(\frac{\sigma_j}{R I_0 \exp\left(-PL\right)}\right)^2} \tag{3}$$

where R is the photodetector responsivity, I_0 is the input laser intensity coupled into the waveguide, P stands for intrinsic waveguide loss not considering the absorption of analyte, L represents the effective absorption length of the waveguide, α is the absorption coefficient of pure analyte, η is the evanescent field fraction in solution, and σ_j denotes dark current noise from the detector. The terms in equation (3) under the square root correspond to two major noise sources: input laser power fluctuation and photodetector noise at the output. The latter term is of influence only when the analyte solution has strong absorption or is highly concentrated as in the case of heavy water absorption coefficient of 18000 cm^{-1} at around 4 μm [12]. In the current system, the former term, fluctuation of laser input power, is about 6% ($\sim$0.26 dB) of optical power effectively passing through the solution. Therefore, the theoretical lowest concentration of IPA in a mixture solution of IPA and acetone that can be sensed by the spiral waveguides is 4.5% for GON platform and 14% for GOS platform, respectively. The experimental measurement results at different concentrations of IPA in IPA-acetone mixtures are shown in Fig. 4.

The lowest volumetric concentration of IPA measured by the sensors on GON and GOS platforms are 5% and 16%, respectively. The experimental measurement results are comparable with the theoretical values which verify that the performance of sensor built on GON platform is better than that of GOS due to its higher evanescent field fraction. The high evanescent field fraction does not sacrifice the propagation loss of the waveguide greatly, owing to the large core-clad index contrast as well as to a transferred Ge layer free of misfit dislocations. This validates the feasibility of using GON as a high performance sensing platform. Lastly, the laser scan (3.65 to 3.90 μm) results, carried out for the spiral waveguide sensor on GON immersed in 100% acetone /100% IPA are shown in the inset of Fig. 4. It is observed that the loss remains the same over most of the range. This is expected as the absorption spectrum of IPA is broad around this wavelength region [29]. For analytes such as IPA or acetic acid [23] whose absorption spectrum is wide, this spiral waveguide can work as a broad band sensor. This chip can also be used for trace gas sensing application with integration to a proper gas sample handling and transporting system as quite a number of gas molecules have their absorption peaks in mid-IR range [24].

4. Conclusion

A spiral waveguide sensor is fabricated on GON platform and demonstrated to have better performance than the GOS platform at nearly the same propagation loss. A high quality Ge layer free of misfit dislocations and a structure with high core-clad index contrast is realized by wafer bonding and layer transfer technique. The GON platform thus developed, assists in designing a waveguide with a high evanescent field fraction to improve absorption based sensitivity while keeping the propagation loss acceptable at the same time. The lowest concentration of IPA in acetone measured in the experiments is 5% for GON vs 16% for GOS, demonstrating the feasibility of using GON as a compact, effective, and accurate platform for mid-IR sensing applications. The sensors fabricated on GON platform can be integrated with a photodetector and a read-out circuit for lab-on-chip applications which can potentially be used in industrial leak detection, process control, medical analysis, and others.

Acknowledgement

References

[1] R. Soref, "Mid-infrared photonics in silicon and germanium," *Nature Photon.*, vol. 4, no. 8, pp. 495–497, 2010.
[2] A. Muraviev *et al.*, "Massively parallel sensing of trace molecules and their isotopologues with broadband subharmonic mid-infrared frequency combs," *Nature Photon.*, vol. 12, pp. 209–214, 2018.
[3] G. Ycas, *et al.*, "High-coherence mid-infrared dual-comb spectroscopy spanning 2.6 to 5.2 μm," *Nature Photon.*, vol. 12, pp. 202–208, 2018.
[4] Y.-C. Chang, *Design, Fabrication and Characterization of Mid-Infrared Strip Waveguide for Laser Spectroscopy in Liquid Environments.* Lausanne, Switzerland: École Polytech. Fédérale de Lausanne, 2012.
[5] B. Behzadi, R. K. Jain, and M. Hossein-Zadeh, "A novel compact and selective gas sensing system based on microspherical lasers," *arXiv preprint arXiv*, vol. 1611, 2016, Art. no. 03855.
[6] R. Kitamura, L. Pilon, and M. Jonasz, "Optical constants of silica glass from extreme ultraviolet to far infrared at near room temperature," *Appl. Opt.*, vol. 46, no. 33, pp. 8118–8133, 2007.
[7] Z. Cheng *et al.*, "Focusing subwavelength grating coupler for mid-infrared suspended membrane waveguide," *Opt. Lett.*, vol. 37, no. 7, pp. 1217–1219, 2012.
[8] Z. Cheng *et al.*, "Mid-infrared suspended membrane waveguide and ring resonator on silicon-on-insulator," *IEEE Photon. J.*, vol. 4, no. 5, pp. 1510–1519, Oct. 2012.
[9] J. S. Penadés *et al.*, "Suspended SOI waveguide with sub-wavelength grating cladding for mid-infrared," *Opt. Lett.*, vol. 39, no. 19, pp. 5661–5664, 2014.
[10] T. Baehr-Jones *et al.*, "Silicon-on-sapphire integrated waveguides for the mid-infrared," *Opt. Exp.*, vol. 18, no. 12, pp. 12127–12135, 2010.
[11] R. Shankar, I. Bulu, and M. Lončar, "Integrated high-quality factor silicon-on-sapphire ring resonators for the mid-infrared," *Appl. Phys. Lett.*, vol. 102, no. 5, 2013, Art. no. 051108.

[12] N. Singh *et al.*, "Mid-IR absorption sensing of heavy water using a silicon-on-sapphire waveguide," *Opt. Lett.*, vol. 41, no. 24, pp. 5776–5779, 2016.

[13] G. Z. Mashanovich *et al.*, "Low loss silicon waveguides for the mid-infrared," *Opt. Exp.*, vol. 19, no. 8, pp. 7112–7119, 2011.

[14] Y.-C. Chang *et al.*, "Cocaine detection by a mid-infrared waveguide integrated with a microfluidic chip," *Lab Chip*, vol. 12, no. 17, pp. 3020–3023, 2012.

[15] B. Troia *et al.*, "Germanium-on-silicon Vernier-effect photonic microcavities for the mid-infrared," *Opt. Lett.*, vol. 41, no. 3, pp. 610–613, 2016.

[16] U. Younis *et al.*, "Germanium-on-SOI waveguides for mid-infrared wavelengths," *Opt. Exp.*, vol. 24, no. 11, pp. 11987–11993, 2016.

[17] M. Sieger *et al.*, "Mid-infrared spectroscopy platform based on GaAs/AlGaAs thin-film waveguides and quantum cascade lasers," *Anal. Chem.*, vol. 88, no. 5, pp. 2558–2562, 2016.

[18] X. Wang *et al.*, "Ultra-sensitive mid-infrared evanescent field sensors combining thin-film strip waveguides with quantum cascade lasers," *Analyst*, vol. 137, no. 10, pp. 2322–2327, 2012.

[19] V. Mere and S. K. Selvaraja, "Germanium-on-glass waveguides for mid-IR photonics," in *Proc. Int. Conf. Fibre Opt. Photon.*, 2016, Art. no. Th3A.18.

[20] M. Nedeljkovic *et al.*, "Surface-grating-coupled low-loss Ge-on-Si rib waveguides and multimode interferometers," *IEEE Photon. Technol. Lett.*, vol. 27, no. 10, pp. 1040–1043, May 2015.

[21] K. Gallacher *et al.*, "Integrated germanium-on-silicon waveguides for mid-infrared photonic sensing chips," in *Proc. 2017 42nd Int. Conf. Infrared Millim. THz Waves*, 2017, pp. 1–2.

[22] K. Gallacher *et al.*, "Germanium-on-silicon waveguides for mid-infrared photonic sensing chips," in *Proc. 2017 IEEE 14th Int. Conf. Group IV Photon.*, 2017, pp. 63–64.

[23] S. Khan *et al.*, "Silicon-on-nitride waveguides for mid-and near-infrared integrated photonics," *Appl. Phys. Lett.*, vol. 102, no. 12, 2013, Art. no. 121104.

[24] A. Z. Subramanian *et al.*, "Silicon and silicon nitride photonic circuits for spectroscopic sensing on-a-chip," *Photon. Res.*, vol. 3, no. 5, pp. B47–B59, 2015.

[25] W. Yan, "Parts-per-trillion moisture measurement using cavity ring-down spectroscopy," *Gases Technol.*, pp. 21–24, Jul./Aug. 2002.

[26] W. Li *et al.*, "Germanium-on-silicon nitride waveguides for mid-infrared integrated photonics," *Appl. Phys. Lett.*, vol. 109, no. 24, 2016, Art. no. 241101.

[27] D. Bartolo *et al.*, "Microfluidic stickers," *Lab Chip*, vol. 8, no. 2, pp. 274–279, 2008.

[28] D. Cai *et al.*, "Raman, mid-infrared, near-infrared and ultraviolet–visible spectroscopy of PDMS silicone rubber for characterization of polymer optical waveguide materials," *J. Mol. Struct.*, vol. 976, nos. 1–3, pp. 274–281, 2010.

[29] E. Sani and A. Dell'Oro, "Spectral optical constants of ethanol and isopropanol from ultraviolet to far infrared," *Opt. Mater.*, vol. 60, pp. 137–141, 2016.

[30] J. Hu *et al.*, "Low-loss integrated planar chalcogenide waveguides for microfluidic chemical sensing," *Proc. SPIE*, vol. 6444, 2007, Art. no. 64440N.